

# Structural properties and electroforming-free resistive switching characteristics of $\text{Nd}_2\text{O}_3$ , $\text{Dy}_2\text{O}_3$ and $\text{Er}_2\text{O}_3$ memory devices fabricated in full room temperature

Ching-Hao Chueh<sup>1</sup>, Chih-Hung Lu<sup>1</sup>, Jim-Long Her<sup>2</sup>, Yasuhiro H. Matsuda<sup>3</sup>, and Tung-Ming Pan<sup>1\*</sup>

<sup>1</sup>Department of Electronic Engineering, Chang Gung University, Taoyuan 333, Taiwan, R. O. C.

<sup>2</sup> Division of Natural Science, Center for General Education, Chang Gung University, Taoyuan 333, Taiwan, R. O. C.

<sup>3</sup>Institute for Solid State Physics, The University of Tokyo, Chiba 277-8581, Japan

\* Tel: +886-3-211-8800 Ext. 3349; Fax: +886-3-211-8507; e-mail: [tspan@mail.cgu.edu.tw](mailto:tspan@mail.cgu.edu.tw)

## 1. Introduction

Resistive-switching random access memory (ReRAM) device, such as NiO, TiO<sub>2</sub>, ZrO<sub>2</sub>, HfO<sub>2</sub> [1-4], etc., is a promising candidate for the next-generation nonvolatile memory, because of its simple structure, low power operation, and high density integration. During the switching process of these oxides, the forming process is often needed to achieve the stable resistive switching (RS) cycles [4]. However, this process usually requires a higher bias and may cause unpredictable resistance states. Up to now, the electroforming-free phenomenon has not been found in the rare-earth (RE) oxide materials.

## 2. Experiment

A ~20 nm RE<sub>2</sub>O<sub>3</sub> thin films were deposited on TaN/SiO<sub>2</sub>/Si substrates at room temperature by means of rf sputtering with a mixture of Ar and O<sub>2</sub> using a metal Nd, Dy, or Er target. In order to measure the electrical characteristics of the RE<sub>2</sub>O<sub>3</sub> films, Ru top electrodes of 200 μm in diameter were deposited at room temperature through dc sputtering with a metal shadow mask. All processing step of Ru/RE<sub>2</sub>O<sub>3</sub>/TaN memory structure was made in RT.

## 3. Results and discussion

A stronger TaN (111) reflection peak was found in the XRD pattern (Fig. 1), but no RE<sub>2</sub>O<sub>3</sub> diffraction peak appeared in the RE<sub>2</sub>O<sub>3</sub>/TaN/SiO<sub>2</sub>/Si structure. This indicates that these RE<sub>2</sub>O<sub>3</sub> thin films are amorphous structure.

Fig. 2 depicts I-V characteristics of the Ru/RE<sub>2</sub>O<sub>3</sub>/TaN ReRAM devices using RE<sub>2</sub>O<sub>3</sub> films. No initial electroforming process is needed for these fresh devices to obtain RS behavior. When the bias is swept from 0 to 4 V, a reproducible unipolar RS behavior is found in these devices. As the voltage went from zero to a positive voltage up to V<sub>set</sub> with a compliance current of 2 mA, the device switched from a high-resistance state (HRS) to a low-resistance state (LRS) and its current increased abruptly. The device kept in the LRS until the voltage was swept from zero to a positive value at V<sub>reset</sub>. When the positive voltage exceeded V<sub>reset</sub>, the device switched back to the HRS again. The Ru/RE<sub>2</sub>O<sub>3</sub>/TaN device using a Dy<sub>2</sub>O<sub>3</sub> film exhibits a higher ratio between HRS and LRS than that of both Nd<sub>2</sub>O<sub>3</sub> and Er<sub>2</sub>O<sub>3</sub> films. Fig. 3 and 4 show the logarithmic plots of the I-V curve for the Ru/RE<sub>2</sub>O<sub>3</sub>/TaN ReRAM devices in the HRS and LRS, respectively. The conduction behavior in the HRS is controlled by Ohm's law a low voltage region due to the straight slope. Furthermore, the conduction behavior in the LRS undergoes Ohmic

transport at because the logarithmic plot of the I-V curve is a linear line with a slope of about 1, as shown in Fig. 4.

The Nd 3d, Dy 4d, and Er 4d spectra, as shown in, demonstrate the coexistence of neodymium ions and metallic Nd<sup>0</sup> in Nd<sub>2</sub>O<sub>3</sub>, the coexistence of dysprosium ions and metallic Dy<sup>0</sup> in Dy<sub>2</sub>O<sub>3</sub>, and the coexistence of erbium ions and metallic Er<sup>0</sup> in Er<sub>2</sub>O<sub>3</sub>. The metallic RE is associated with the conductive filament. In addition, the O 1s spectra of Nd<sub>2</sub>O<sub>3</sub>, Dy<sub>2</sub>O<sub>3</sub>, and Er<sub>2</sub>O<sub>3</sub> films, as shown in Fig. 6(a)-(c), indicate the composition of lattice oxygen ions (O at 529.5 eV) and nonlattice oxygen ions (O at 532.4 eV) in Nd<sub>2</sub>O<sub>3</sub>, lattice oxygen ions (O at 529.4 eV) and nonlattice oxygen ions (O at 531.9 eV) in Dy<sub>2</sub>O<sub>3</sub>, and lattice oxygen ions (O at 529.7 eV) and nonlattice oxygen ions (O at 532.2 eV) in Er<sub>2</sub>O<sub>3</sub> [5]. The formation of conductive filaments should be attributed to the localized agglomeration of the oxygen vacancies (V<sub>O</sub><sup>2+</sup>) in RE<sub>2</sub>O<sub>3</sub> film, by analogy with the metallic Re, as shown in Fig. 7. We describe a microscopic model of filament formation and rupture for the Ru/RE<sub>2</sub>O<sub>3</sub>/TaN by employing the stable vacancy states.

Fig. 8 shows the retention of the Ru/RE<sub>2</sub>O<sub>3</sub>/TaN device at 0.5 V read-out. Both HRS and LRS for the Dy<sub>2</sub>O<sub>3</sub> and Er<sub>2</sub>O<sub>3</sub> films are almost kept at the same resistance values without any observable degradation at 25°C. Consequently, these devices exhibit nondestructive readout and good reliability. The endurance characteristics of the Ru/RE<sub>2</sub>O<sub>3</sub>/TaN devices are shown in Fig. 9. The resistance ratio between two states for the Dy<sub>2</sub>O<sub>3</sub> film is still more than 110. In contrast, the Ru/Nd<sub>2</sub>O<sub>3</sub>/TaN ReRAM device exhibited the unstable RS behavior and switching cycle less than 30.

## 4. Conclusions

The RS characteristics of Ru/RE<sub>2</sub>O<sub>3</sub>/TaN memory devices with full room temperature process have been demonstrated. The dominant conduction mechanisms of LRS and HRS are Ohmic behavior. The Ru/Dy<sub>2</sub>O<sub>3</sub>/TaN ReRAM memory device has the characteristics of no-electroforming process, high resistance ratio, good data retention and endurance. This memory device is very promising candidate for future nonvolatile ReRAM memory applications.

## References

- [1] B. J. Choi et al., J. Appl. Phys. 98, 033715 (2005).
- [2] Y. Li et al., IEEE Electron Device Lett. 31, 117 (2010).
- [3] K. L. Lin et al., J. Appl. Phys. 109, 084104 (2011).
- [4] R. Waser et al., Adv. Mater. 21, 2632 (2009).
- [5] Y. Uwamino et al., J. Electron Spectrosc. Relat. Phenom. 34, 67 (1984).

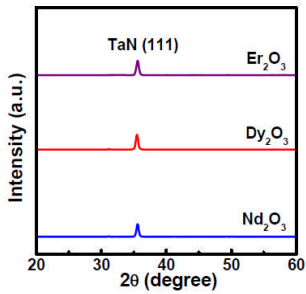


Fig. 1. XRD patterns of  $\text{Nd}_2\text{O}_3$ ,  $\text{Dy}_2\text{O}_3$  and  $\text{Er}_2\text{O}_3$  thin films.

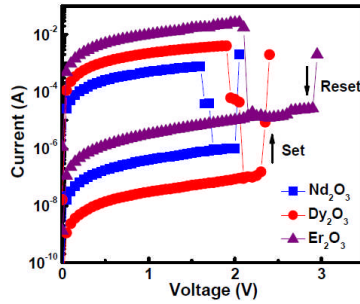


Fig. 2. Type I-V curves of resistive switching behavior in the  $\text{Ru}/\text{RE}_2\text{O}_3/\text{TaN}$  ReRAM devices using  $\text{Nd}_2\text{O}_3$ ,  $\text{Dy}_2\text{O}_3$  and  $\text{Er}_2\text{O}_3$  thin films.

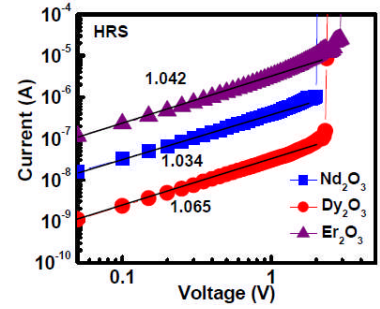


Fig. 3. The conducting mechanisms of HRS in the  $\text{Ru}/\text{RE}_2\text{O}_3/\text{TaN}$  ReRAM devices.

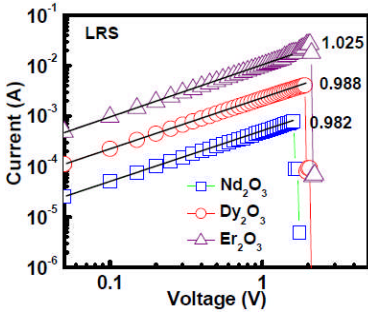


Fig. 4. The conducting mechanisms of LRS in the  $\text{Ru}/\text{RE}_2\text{O}_3/\text{TaN}$  ReRAM devices.

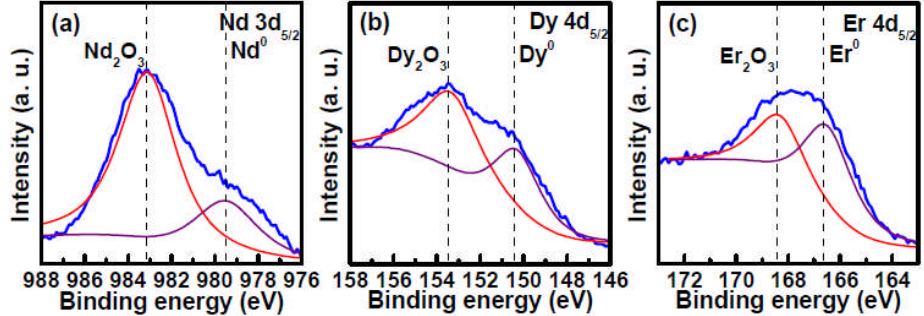


Fig. 5. (a) Nd 3d, (b) Dy 4d and (c) Er 4d XPS spectra of  $\text{RE}_2\text{O}_3$  dielectric films deposited on  $\text{TaN}/\text{SiO}_2/\text{Si}$  substrates.

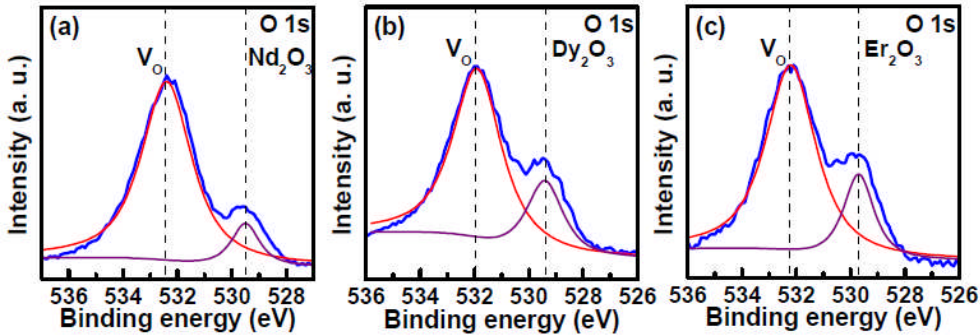


Fig. 6. (a)-(c) O 1s XPS spectra of  $\text{RE}_2\text{O}_3$  dielectric films deposited on  $\text{TaN}/\text{SiO}_2/\text{Si}$  substrates.

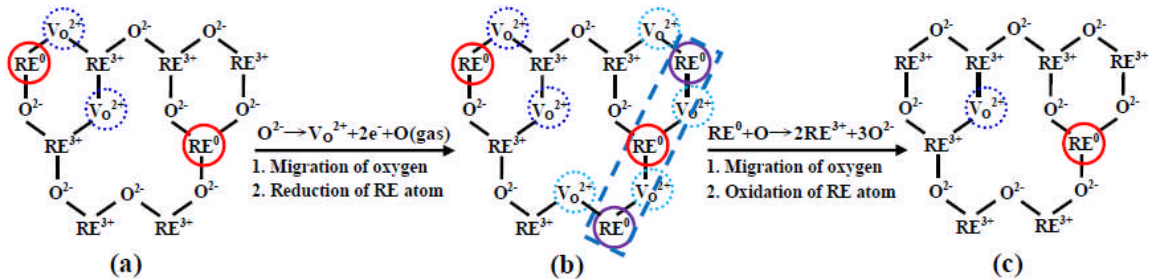


Fig. 7. Schematic diagram of resistance switching mechanism in  $\text{RE}_2\text{O}_3$  thin films for (a) conduction, (b) formation, and (c) rupture of filament. The pre-existing conduction filaments consist of metallic RE ( $\text{RE}^0$ , red color solid) and oxygen vacancies ( $\text{V}_\text{O}^{2+}$ , blue color dash) in the  $\text{RE}_2\text{O}_3$  film. The formation of the filaments is due to oxygen ions migration in RE-O bonds producing oxygen vacancy ( $\text{V}_\text{O}^{2+}$ , light blue color dash) and the reaction of two electrons with RE atoms forming metallic RE ( $\text{RE}^0$ , purple color solid), causing  $\text{RE}^0$  atoms connected in a chain (light royal color dash).

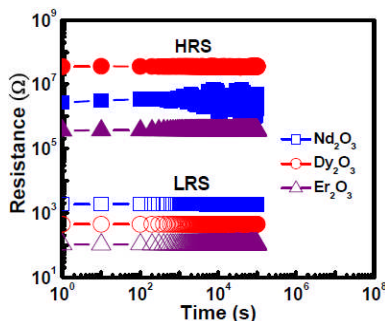


Fig. 8. Retention characteristics of the  $\text{Ru}/\text{RE}_2\text{O}_3/\text{TaN}$  devices in both resistance states.

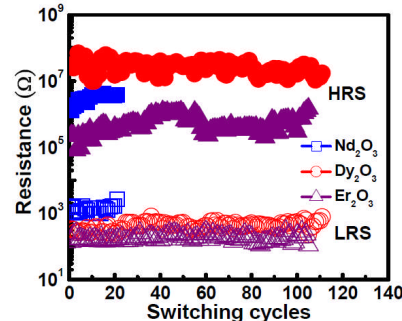


Fig. 9. Resistance values of both HRS and LRS versus cycle numbers for  $\text{Ru}/\text{RE}_2\text{O}_3/\text{TaN}$  devices.